Magnetic fields from compensated isocurvature perturbations

Jordan Flitter[*]

Physics Department, Ben-Gurion University of the Negev, Beer-Sheva 84105, Israel

Cyril Creque-Sarbinowski

Center for Computational Astrophysics, Flatiron Institute, 162 Fifth Avenue,
New York, New York 10010, USA

Marc Kamionkowski

William H. Miller III Department of Physics and Astronomy, Johns Hopkins University,
Baltimore, Maryland 21218, USA

Liang Dai

Department of Physics, University of California, 366 Physics North MC 7300,
Berkeley, California 94720, USA

Compensated isocurvature perturbations (CIPs) are perturbations to the primordial baryon density that are accompanied by dark-matter-density perturbations so that the total matter density is unperturbed. Such CIPs, which may arise in some multifield inflationary models, can be long-lived and only weakly constrained by current cosmological measurements. Here we show that the CIP-induced modulation of the electron number density interacts with the electron-temperature fluctuation associated with primordial adiabatic perturbations to produce, via the Biermann-battery mechanism, a magnetic field in the post-recombinaton Universe. Assuming the CIP amplitude saturates the current BBN bounds, this magnetic field can be stronger than 10^{-15} nG at $z \simeq 20$ and stronger by an order of magnitude than that (produced at second order in the adiabatic-perturbation amplitude) in the standard cosmological model, and thus can serve as a possible seed for galactic dynamos.

I. INTRODUCTION

Our current cosmological model is consistent with the idea of a period of inflationary expansion in the early Universe that generated the primordial density perturbations that seeded the growth of cosmic large-scale structure. The canonical model is, however, no more than a toy model, and so efforts are aimed to seek new relics in primordial perturbations, beyond the nearly scale-invariant Gaussian adiabatic perturbations predicted in the simplest models. Possibilities include various types of non-Gaussianity, departures from scale invariance, and assorted type of isocurvature perturbations [1–14].

Included among these possibilities are compensated isocurvature perturbations (CIPs), perturbations to the dark-matter density that are compensated by baryon-density perturbations in such a way that the isocurvature part of the total matter perturbation vanishes [15–17]. CIPs, which can arise in some multi-field models [15,16,18–22] or during baryogenesis [23] are particularly intriguing as

CIPs induce (at linear order) no temperature fluctuations in the cosmic microwave background (CMB). The fluctuations remain frozen until shortly after recombination due to CMB drag. The subsequent evolution is triggered by the baryon-gas pressure, which is small, thus affecting perturbations only on very small scales. Constraints to CIPs on large scales come from higher-order effects on the CMB power spectrum [24–28] and the CMB trispectrum [29–31] while CIPs on small distance scales may be manifest in CMB spectral distortions [32,33] or the recombination history [34]. Still, these effects arise only at higher order in perturbation theory and so are fairly weakly constrained. The effects of CIPs have also been considered for baryon acoustic oscillations [35–37]; 21-cm fluctuations [16]; velocity acoustic oscillations [38,39] in the 21-cm power spectrum [40]; scale-dependent bias [41,42]; and kSZ tomography [43–45].

Here we show that CIPs induce magnetic fields by interacting with primordial adiabatic perturbations during the dark ages, after recombination but before the epoch of reionization. The CIP gives rise to an isothermal perturbation to the electron number density that then interacts, via

---
[*]jordanf@post.bgu.ac.il

the Biermann-battery mechanism [46], with the electron-temperature gradients associated with the adiabatic perturbation to generate a magnetic field. A similar mechanism operates in the standard cosmological model at second order in the adiabatic-density-perturbation amplitude [46] and generates magnetic fields weaker than $\mathcal{O}(10^{-15} \text{ nG})$ at the redshifts, $z \simeq 20$, at which the first structures become nonlinear. As the CIP amplitude may be four orders of magnitude larger than the adiabatic-perturbation amplitude, one might expect that the CIPs can induce magnetic fields of order 10^{-11} nG at redshifts $z \sim 20$ and thus possibly detectable by 21-cm measurements [47,48]. Yet, our analysis shows that cancelations in the amplitude of the fluctuations in the electron number-density suppress that enhancement.

The remaining parts of this paper are organized as follows. In Sec. II we discuss large- and small-scale constraints on the CIP amplitude and relate those to the amplitude of the CIPs-induced free-electron-density fluctuations. We then derive, in Sec. III, the magnetic fields that could have arisen from the CIPs. We conclude with a discussion on our results in Sec. IV.

In this work we have adopted the cosmological parameters from the best-fit of Planck 2018 [49], that is a Hubble constant $h = 0.6736$, a primordial curvature amplitude $A_s = 2.1 \times 10^{-9}$ with a spectral index $n_s = 0.9649$, and total matter and baryons density parameters $\Omega_m = 0.3153$, $\Omega_b = 0.0493$.

II. COMPENSATED ISOCURVATURE PERTURBATIONS

We describe the CIP field $\Delta(\mathbf{x}) = \delta\rho_b(\mathbf{x})/\bar{\rho}_b$ to be the isocurvature fractional perturbation to the baryon density. This field is then accompanied by a fractional isocurvature perturbation $\delta\rho_c(\mathbf{x})/\bar{\rho}_c = -f_b\Delta(\mathbf{x})$ to the cold-dark-matter density, where $f_b = \Omega_b/\Omega_c$ is the ratio of the baryon and dark-matter densities. We take the primordial CIP field to be a realization of a random field with a power spectrum $\propto k^\alpha$ with the wave number k. The time evolution of the CIP field is simple. The absence of any density perturbation implies no curvature perturbations (at least at linear order) and thus no gravitational acceleration. The pressure gradients in the baryon-photon fluid introduced by the baryon fluctuation are extremely small. The baryon isocurvature perturbation then remains frozen through radiation drag, which ends at redshift $z \simeq 800$, when the baryon temperature is roughly 0.2 eV and the baryon sound speed thus $c_s \sim 1.3 \times 10^{-5}c$. At this point, the baryons then spread out at the sound speed, thus smoothing fluctuations on comoving distance scales smaller than $\sim 2 \times 10^{-2}$ Mpc, comparable to the Jeans scale.

If the power-law index $\alpha > -3$, then the perturbations are largest at small wavelengths (high k). If the perturbation amplitude is large, it will affect the agreement between observed light-element abundances and the predictions of big-bang nucleosynthesis (BBN). If the dependence of light-element abundances on the baryon density is perfectly linear, then there will be no change to the abundances after averaging over small-scale fluctuations. The dependence of the deuterium abundance on the baryon density is, however, not linear; it is approximated by $(D/H) \propto \Omega_b^{-3/2}$ [50]. Tthe deuterium abundance will thus be shifted at quadratic order in Δ by $(1 + \Delta)^{-3/2} \approx 1 - \frac{3}{2}\Delta + \frac{15}{8}\Delta^2$, and after averaging over many small-scale fluctuations the fractional variation in the deuterium abundance is $\delta(D/H)/\overline{(D/H)} \sim 2\langle\Delta^2\rangle$. The $\sim 1\%$ precision of the current deuterium abundance [51] then suggests $\langle\Delta^2\rangle \lesssim 5 \times 10^{-3}$.

If on the other hand $\alpha \leq -3$, the baryon density is smooth on small scales but varies on large scales. The rapid Compton interactions prior to recombination will imprint these large scales fluctuations in the baryon density field into large scales fluctuations in the CMB, which would be observed as a difference between the CMB power spectrum on one half of the sky and that on the other half. Current CMB constraints indicate that $\langle\Delta^2\rangle \lesssim 4 \times 10^{-3}$ [28].

The Biermann-battery mechanism will depend on the fractional free-electron-density perturbation $\delta_e(\mathbf{x}) \equiv \delta n_e(\mathbf{x})/\bar{n}_e$. The free-electron-density n_e at any given point in the post-recombination Universe will be the product of the baryon density and the free-electron fraction x_e. After recombination, the free-electron fraction is proportional to $(1 + \Delta)^{-1.05}$ (for small values of Δ), an approximation that we have verified with detailed calculations from HYREC [52,53]). Due to an $\mathcal{O}(\%1)$ correction from the helium abundance [50], the induced electron-density perturbation by the CIPs is therefore

$$\delta_e(\mathbf{x}) \approx -0.06\Delta(\mathbf{x}) \equiv -\xi\Delta(\mathbf{x}), \tag{1}$$

as we have verified numerically with HYREC, see Fig. 1. Ultimately, the suppression by ξ will generate weaker magnetic fields, even though the CIP amplitude can be four orders of magnitude stronger than the adiabatic perturbations.

For simplicity, we will take the free-electron power spectrum to be in the form of a power law,

$$P_e(k) = A_e k_{\max}^{-3}(k/k_{\max})^\alpha \Theta(k_{\max} - k)\Theta(k - k_{\min}), \tag{2}$$

parameterized in terms of an amplitude A_e and power-law index α. For a slow-roll inflation, a scale-invariant CIP power-spectrum is usually considered (with $\alpha = -3$), a choice that is also consistent with the latest Planck CMB analysis [28]. Here we work with a general index α to allow comparison of our results with other CIP probes in the literature. In our model, the CIPs power vanishes at Fourier modes below $k_{\min}$, which essentially corresponds to the horizon scale, and above $k_{\max}$. For $k_{\max}$ we shall adopt as our fiducial value the Jeans scale at the end of the drag epoch, i.e. $k_{\max} \sim 400$ Mpc^{-1}.
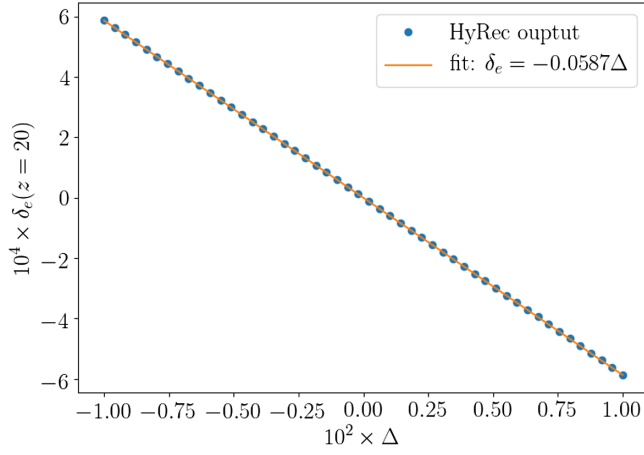
FIG. 1. Fluctuations in the fractional free-electron-density at $z = 20$ as a function of the CIP amplitude. This figure was made by running CLASS [54] (which inherently runs HYREC) with different values of Ω_b and Ω_c that are controlled by the CIP amplitude Δ. As CLASS and HYREC return n_e/n_H, where n_H is the hydrogen-number-density, that quantity was multiplied by $n_H \propto \Omega_b(1 - Y_{He})$, where Y_{He} is the helium-mass-ratio (a quantity that is interpolated by CLASS given the cosmological parameters).

The BBN bound on $\langle \Delta^2 \rangle$ implies an electron-density variance $\langle \delta_e^2 \rangle = (2\pi^2)^{-1} \int k^2 dk P_e(k) \lesssim 5 \times 10^{-3}\xi^2$. We thus constrain

$$A_e \lesssim (5 \times 10^{-3}\xi^2) \times 2\pi^2(3 + \alpha) \qquad (\alpha > -3). \quad (3)$$

To derive the CMB bounds on A_e, we consider the CIP variance, smoothed on a sphere of radius R,

$$\langle \Delta^2 \rangle_R = \frac{1}{2\pi^2} \int k^2 dk \left[\frac{3j_1(kR)}{kR} \right]^2 P_\Delta(k), \qquad (4)$$

where $j_1(x)$ is the spherical Bessel function of order 1. The CIPs power spectrum is obtained from Eq. (1), $P_\Delta(k) = \xi^{-2} P_e(k)$. By taking $R = R_{CMB} \sim 125$ Mpc [26,45], the CMB constraints on the CIP variance imply

$$A_e \lesssim (4 \times 10^{-3}\xi^2)/I_\alpha \quad (\alpha \leq -3), \quad (5)$$

where

$$I_\alpha = \frac{1}{2\pi^2} \int_{k_{min}}^{k_{max}} \frac{k^{2+\alpha} dk}{k_{max}^{3+\alpha}} \left[\frac{3j_1(kR_{CMB})}{kR_{CMB}} \right]^2. \quad (6)$$

III. BIERMANN BATTERY MECHANISM

We now consider the magnetic fields produced in the postrecombination Universe by the interaction of electron-density fluctuations, with $k \leq k_{max}$, with primordial adiabatic density perturbations. In the standard cosmological

model these density perturbations are characterized by the ΛCDM power spectrum. Right after recombination, the growth of perturbations to the baryon density are suppressed by Compton drag, but at later times, $z \lesssim 800$, the baryons freely fall and later acquire the same distribution as dark matter, but only for Fourier modes with wavelengths longer than the baryon Jeans scale [55]. The gas is adiabatic and so baryon-temperature perturbations (and thus electron-temperature perturbations) have an amplitude $2/3$ times the density-perturbation amplitude. This linear-theory evolution proceeds until a redshift $z \sim 20$ at which point fluctuations are suppressed at scales smaller than the Jeans scale[1,2] $k_J \simeq 200$ Mpc^{-1}. We thus here calculate the generation of magnetic fields at redshifts $20 \lesssim z \lesssim 800$ after baryon drag and before nonlinear structures form. Nonlinear evolution is likely to amplify the magnetic fields, perhaps considerably, and so the magnetic-field strengths we obtain should be considered conservative lower bounds.

Magnetic fields are generated in the Biermann-battery mechanism if there is a component of the gradient of the electron temperature that is perpendicular to the gradient of the electron density. The evolution of the cosmic magnetic field $\mathbf{B}$ is related to the electric field $\mathbf{E}$ through Faraday's law, $\partial \mathbf{B}/\partial t = -c\nabla \times \mathbf{E}$, with c being the speed of light. Taking the pressure term to be the dominant term in the generalized Ohm's law [57], the electric field is $\mathbf{E} = -\nabla p_e/(n_e e)$, where p_e is the electron pressure and e is the electron charge. Accounting for the expansion of the Universe, the evolution of the magnetic field is then [58]

$$\frac{d}{dt}(a^2 \mathbf{B}) = -\frac{c}{en_e^2}\nabla n_e \times \nabla p_e$$

$$= -\frac{ck_B}{en_e}\nabla n_e \times \nabla T, \quad (7)$$

where $a(t)$ is the scale factor and the second line follows the equation of state of collisionless electrons, $p_e = n_e k_B T$, with k_B the Boltzmann constant and T the electron temperature. After defining $\delta_T \equiv \delta T/\bar{T}$ to be the fractional electron-temperature perturbation and $\bar{T}$ the mean electron temperature (which we take to be the mean baryon temperature), in the lowest order of perturbation theory we arrive at [46]

---

[1]Strictly speaking, the comoving Jeans scale at $z = 20$ is ~ 900 Mpc^{-1}. To reduce clutter though, we refer to $k_J \simeq 200$ Mpc^{-1} as the scale where the temperature fluctuations are suppressed by k^{-2} compared to the baryons-density fluctuations [56].

[2]In addition, in our analysis we neglect effects from the relative velocity between baryons and cold-dark-matter v_{bc}. We anticipate, based on the treatment in Ref. [46], the including of v_{bc} would result an $\mathcal{O}(1)$ correction of the induced magnetic field, as well as to an extension of the magnetic field power spectrum to larger wave numbers.

$$\frac{d}{dt}(a^2\mathbf{B}) = -\frac{ck_B\bar{T}}{e}\nabla\delta_e \times \nabla\delta_T. \tag{8}$$

The Fourier components $\tilde{\mathbf{B}}(\mathbf{k},t)$ of the magnetic field induced between some initial time t_i and time t are given by

$$\tilde{\mathbf{B}}(\mathbf{k},t) = \frac{ck_B}{a^2(t)e}\int_{t_i}^{t}dt'\bar{T}(t')$$
$$\times \int\frac{d^3k_1}{(2\pi)^3}[\mathbf{k}_1 \times (\mathbf{k}-\mathbf{k}_1)]\tilde{\delta}_e(\mathbf{k}_1,t')\tilde{\delta}_T(\mathbf{k}-\mathbf{k}_1,t'). \tag{9}$$

As there is no gravitational attraction in the linear order of the CIP theory, we approximate the electron isocurvature-density fluctuation as constant in time over the relevant wavelengths after recombination, and the electron-temperature perturbation scales as the linear-theory growth factor $D(z)$ (normalized to unity today) which varies as $D(z) \propto 1/(1+z)$ over the relevant redshifts. The electron temperature $\bar{T}(z) \propto (1+z)^2$ and the time is $t \simeq (2/3)(\Omega_m H_0^2)^{-1/2}(1+z)^{-3/2}$ at these redshifts. The redshift (or time) dependence then factorizes and allows us to write the magnetic-field power spectrum at redshift z as

$$P_B(k,z) = [F_B(z)]^2 \int\frac{d^3k_1}{(2\pi)^3}[\mathbf{k}_1 \times (\mathbf{k}-\mathbf{k}_1)]^2$$
$$\times P_e(k_1)P_T(|\mathbf{k}-\mathbf{k}_1|), \tag{10}$$

where

$$F_B(z) = \frac{2ck_B\bar{T}(z)D(z)}{e\sqrt{\Omega_m}H_0}(1+z)^{1/2}. \tag{11}$$

The scalings of $\bar{T}(z)$ and $D(z)$ with z imply that $F_B(z) \propto (1+z)^{3/2}$. This scaling is slower than the $(1+z)^2$ scaling for a static comoving magnetic field, indicating that the comoving magnetic field is generated primarily at late times. Our rough treatment of the evolution of the baryon temperature at early times is thus justified and we hereafter adopt $k_{\min} = 3 \times 10^{-4}$ Mpc^{-1}, corresponding to the horizon scale at $z = 20$. Numerically, the baryon temperature is $\bar{T}(z=20) \simeq 10$ K, and $D(z=20) \simeq 0.06$, and then

$$F_B(z) \simeq 4.1 \times 10^{-27} \text{ G Mpc}^2 \left(\frac{1+z}{21}\right)^{3/2}. \tag{12}$$

The magnetic-field variance then becomes

$$\langle\mathbf{B}^2\rangle = \int\frac{d^3k}{(2\pi)^3}P_B(k)$$
$$= [F_B(z)]^2\langle\sin^2\theta\rangle$$
$$\times \left[\int\frac{d^3k}{(2\pi)^3}k^2P_e(k)\right]\left[\int\frac{d^3k}{(2\pi)^3}k^2P_T(k)\right], \tag{13}$$

where $\langle\sin^2\theta\rangle = 2/3$ is the angle between $\mathbf{k}_1$ and $\mathbf{k}$ averaged over all directions. The first integral in Eq. (13) evaluates to $A_e k_{\max}^2[2\pi^2(5+\alpha)]^{-1}|1-(k_{\min}/k_{\max})^{\alpha+5}|$. We evaluate the second integral using CLASS [54], cutting off the integral at the Jeans scale $k_J \simeq 200$ Mpc. It comes out to $2.2 \times 10^5(k_J/200 \text{ Mpc}^{-1})^2$ Mpc^{-2}, where the scaling with k_J arises given that the integral is dominated by the high-k limit where $P_m(k)$ varies very slowly with k.

We thus find an rms magnetic-field strength

$$\langle\mathbf{B}^2\rangle^{1/2} \simeq 2.9 \times 10^{-15} \text{ nG}\left(\frac{A_e}{(2\times10^{-5})2\pi^2|5+\alpha|}\right)^{1/2}$$
$$\times \frac{k_J}{200 \text{ Mpc}^{-1}}\frac{k_{\max}}{400 \text{ Mpc}^{-1}}\left(\frac{1+z}{21}\right)^{3/2}$$
$$\times \left|1-\left(\frac{k_{\min}}{k_{\max}}\right)^{5+\alpha}\right|^{1/2}, \tag{14}$$

at redshifts $z \simeq 20$. A few comments: (1) The scaling with redshift is expected to break down for redshifts $z \lesssim 20$ for several reasons. First, small-scale perturbations will go nonlinear, violating the assumption of linearity. Second, the formation of stars will heat the gas and increase the temperature. Moreover, we expect that the motions of magnetized gas that winds up in gravitationally bound systems will lead, through the dynamo mechanism, to magnetic fields within halos that are far stronger than the seed fields provided by our analysis. (2) The behavior of the small-scale power spectrum, on scales smaller than the Jeans scale, can be calculated, as we show in the appendix. Here we have modeled it as a strict cutoff for simplicity and to help indicate the uncertainty on this small-scale physics. Yet, we find that Eq. (14) is accurate to the order of $\mathcal{O}(10\%)$ when we compare it to numerical calculations with a more refined modeling of the suppression at small scales, as we discuss next.

IV. DISCUSSION

In Fig. 2 we plot the magnetic-field power spectrum for values of $-5 \leq \alpha \leq 5$, in each case taking A_e to be the maximum value allowed by the BBN constraint for $\alpha > -3$ [Eq. (3)] and by the CMB bound for $\alpha < -3$ [Eq. (5)]. As above, the CIP power spectrum is assumed here to be cut off at $k_{\max} = 400$ Mpc^{-1}; this cutoff gives rise to the sharp drop in $P_B(k)$ at this value of k, mostly evident at $\alpha = -5$. In this calculation, though, we use the standard ΛCDM power spectrum from CLASS [54], with best-fit Planck cosmological parameters [49]. We then extend it to smaller scales (higher k) with the BBKS approximation [59] with the baryon correction of Ref. [60]. We then continue the matter power spectrum to $k > k_J$, above the Jeans scale, with a suppression $(k/k_J)^{-4}$ [55,56], for $k > k_J = 200$ Mpc^{-1}, relative to the BBKS power spectrum.
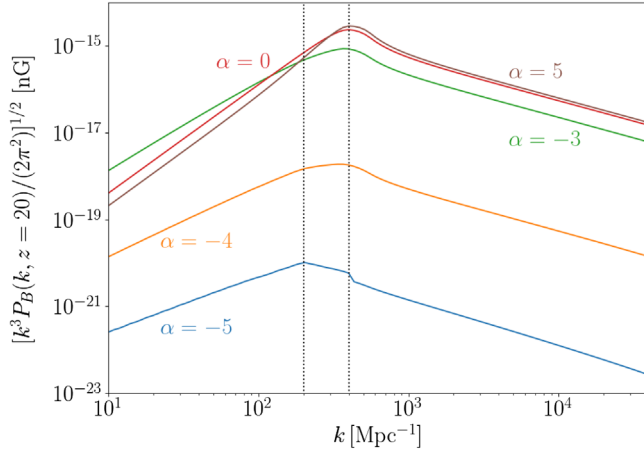
FIG. 2. The magnetic-field power spectrum as a function of wave number for different values of the electron-density spectral index α. For values of $\alpha > -3$ ($\alpha \leq -3$), the normalization of the CIP power spectrum is taken to be the maximum allowed by the BBN (CMB) constraint, Eq. (3) [Eq. (5)]. The vertical lines indicate the assumed Jeans wave number $k_J = 200$ Mpc^{-1} and the cutoff $k_{\max} = 400$ Mpc^{-1} in the electron-density power spectrum.

The magnetic-field power peaks in all cases at $k \simeq k_{\max}$, but is a bit more broadly distributed to lower k for $\alpha < -3$ (see derivation in the appendix for the power-law behavior at small and large scales). For $\alpha > 0$ the power at the vicinity of $k \sim k_{\max}$ surpasses 10^{-15} nG. In all cases, the magnetic-field energy density is negligible compared with the thermal energy density in the gas at these redshifts (this would require $B \sim$ nG), and so it is dynamically unimportant. It also follows, from this figure, that this mechanism is not constrained by upper limits of $\sim$nG to intergalactic magnetic fields [61–63] nor strong enough to be relevant for the magnetic fields suggested by interpretation of variability of gamma-ray sources [64–66], which reach as small as $B \sim 10^{-8}$ nG. If the CIP amplitude is close to its BBN upper bounds, as we have assumed in this calculation, the field strengths may be suitable to account for seed fields for galactic dynamos [67], which in some models can be as small as 10^{-21} nG at the time of galaxy formation [68]. The magnetic-field strengths we obtain can be higher than those that arise at quadratic order in the primordial density perturbation [46].

In conclusion, in this work we have studied the spectrum and strength of magnetic fields that could have been generated via the Biermann-battery mechanism, where the fluctuations in the electron number-density are sourced by the CIP field. Our main result is Eq. (14). As a first study on this effect, we favored simplicity over precision in order to estimate the strength of the CIP-induced magnetic fields. Although the analysis presented in this paper can be improved by performing a full perturbation analysis that includes also the relative velocity between baryons and

cold-dark-matter, as was done in Ref. [46], we do not expect these improvements to alter the qualitative features of the magnetic fields we obtained, certainly not by orders of magnitude.

At first, one may have surmised that CIP-induced magnetic fields could be up to a few orders of magnitude larger, given that the CIP amplitude can be orders of magnitude larger than the adiabatic-perturbation amplitude. Much of that gain is erased, however, by the near cancellation between the fluctuations in the free-electron fraction and the baryon density in the CIP. Our calculation shows that, when all the dust has settled, the CIP allows for a larger magnetic field, but not much.

APPENDIX: ANALYTICAL APPROXIMATIONS FOR THE MAGNETIC FIELD POWER SPECTRUM

Equation (10) can written in the following form,

$$P_B(k) = [F_B(z)]^2 I(k), \qquad (A1)$$

where

$$
\begin{aligned}
I(k) &= \int \frac{d^3 k_1}{(2\pi)^3} |\mathbf{k}_1 \times \mathbf{k}|^2 P_e(k_1) P_T(|\mathbf{k} - \mathbf{k}_1|) \\
&= \frac{A_e k^{7+\alpha}}{4\pi^2 k_{\max}^{3+\alpha}} \int_{-1}^{1} d\mu (1 - \mu^2) I_x(k, \mu),
\end{aligned} \qquad (A2)
$$

and

$$I_x(k, \mu) = \int_{x_{\min}}^{x_{\max}} dx\, x^{4+\alpha} P_T[k\beta(x, \mu)], \qquad (A3)$$

where $\beta(x, \mu) = \sqrt{1 + x^2 - 2x\mu}$, $x_{\min} \equiv k_{\min}/k$ and $x_{\max} \equiv k_{\max}/k$. For simplicity, we model the temperature power spectrum as follows

$$P_T(k) = \frac{4}{9} P_m(k) \times \begin{cases} 1 & k \leq k_J \\ x_J^4 & k \geq k_J \end{cases}, \qquad (A4)$$

where $P_m(k)$ is the linear matter power spectrum and $x_J \equiv k_J/k$.

Below we examine $I(k)$ in two limits. Throughout the derivation, we assume $k \gg k_{eq} \approx 0.01$ Mpc^{-1} and assume that the matter power spectrum scales as $P_m(k) \propto k^{n_s-4}$ (we ignore small logarithmic corrections). We also assume that k_J and k_{max} are of the same order and limit ourselves to $\alpha \geq -5$. The final expressions for $I(k)$, Eqs. (A11) and (A14) capture very well the power-laws behavior seen in Fig. 2 and provide a good order of magnitude estimation.

1. First limit: $k \ll k_J < k_{max}$ ($1 \ll x_J < x_{max}$)

In the limit where $x_{max} \gg 1$, we split the integral of $I_x(k,\mu)$ into two regimes, $I_x(k,\mu) = I_x^{x_{min}\to 1}(k,\mu) + I_x^{1\to x_{max}}(k,\mu)$. For the first piece, $I_x^{x_{min}\to 1}(k,\mu)$, we approximate $\beta(x,\mu) \approx 1$, which yields

$$
\begin{aligned}
I_x^{x_{min}\to 1}(k,\mu) &= \frac{4}{9} P_m(k) C_\alpha^{(1)}(k) \\
&\approx \frac{4}{9} P_m(k_{max}) C_\alpha^{(1)}(k) x_{max}^{4-n_s}.
\end{aligned}
\tag{A5}
$$

where $C_\alpha^{(1)}(k)$ is an $\mathcal{O}(1)$ factor (assuming $\alpha \geq -5$)

$$
C_\alpha^{(1)}(k) = \begin{cases} \frac{1-x_{min}^{5+\alpha}}{5+\alpha} \approx \frac{1}{5+\alpha} & \alpha + 5 \neq 0 \\ -\ln x_{min} & \alpha + 5 = 0 \end{cases}.
\tag{A6}
$$

For the second piece, $I_x^{1\to x_{max}}(k,\mu)$, we approximate $\beta(x,\mu) \approx x$. Thus, in the range $1 \leq x \leq x_{max}$,

$$
\begin{aligned}
P_T[k\beta(x,\mu)] &\approx \frac{4}{9} P_m(k_{max}) \left(\frac{x}{x_{max}}\right)^{n_s-4} \\
&\times \begin{cases} 1 & 1 \leq x \leq x_J \\ (x/x_J)^{-4} & x_J \leq x \leq x_{max} \end{cases},
\end{aligned}
\tag{A7}
$$

Then, the calculation of $I_x^{1\to x_{max}}(k,\mu)$ is straightforward,

$$
I_x^{1\to x_{max}}(k,\mu) = \frac{4}{9} P_m(k_{max}) C_\alpha^{(2)} \begin{cases} x_{max}^{\alpha+5} & \alpha+n_s+1 \geq 0 \\ x_{max}^{4-n_s} & \alpha+n_s+1 < 0 \end{cases},
\tag{A8}
$$

where $C_\alpha^{(2)}$ is another $\mathcal{O}(1)$ constant,

$$
C_\alpha^{(2)} = \begin{cases} \frac{(\alpha+n_s+1)x_{max/J}^{\alpha+n_s-3}-4}{(\alpha+n_s+1)(\alpha+n_s-3)} x_{max/J}^{\alpha+n_s+1} & \alpha+n_s+1 > 0 \\ \ln x_J + \frac{1-x_{max/J}^{-4}}{4} & \alpha+n_s+1 = 0 \\ -\frac{1}{\alpha+n_s+1} & \alpha+n_s+1 < 0 \end{cases},
\tag{A9}
$$

where $x_{max/J} \equiv x_{max}/x_J = \mathcal{O}(1)$.

Because $x_{max} \gg 1$, $x_{max}^{\alpha+5} \gg x_{max}^{4-n_s}$ for $\alpha+n_s+1 \geq 0$ and therefore $I_x^{1\to x_{max}} \gg I_x^{x_{min}\to 1}$, while $I_x^{1\to x_{max}}$ and $I_x^{x_{min}\to 1}$ are comparable for $\alpha+n_s+1 < 0$. Thus

$$
\begin{aligned}
I_x(k,\mu) &= \frac{4}{9} P_m(k_{max}) \\
&\times \begin{cases} C_\alpha^{(2)} x_{max}^{\alpha+5} & \alpha+n_s+1 \geq 0 \\ (C_\alpha^{(1)}(k) + C_\alpha^{(2)}) x_{max}^{4-n_s} & \alpha+n_s+1 < 0 \end{cases},
\end{aligned}
\tag{A10}
$$

Since $I_x(k,\mu)$ does not depend on μ, the μ integral in Eq. (A2) gives $4/3$, and we have

$$
I(k) = A_B \begin{cases} C_\alpha^{(2)} \left(\frac{k}{k_{max}}\right)^2 & \alpha+n_s+1 \geq 0 \\ (C_\alpha^{(1)}(k) + C_\alpha^{(2)})\left(\frac{k}{k_{max}}\right)^{\alpha+n_s+3} & \alpha+n_s+1 < 0 \end{cases},
\tag{A11}
$$

where

$$
\begin{aligned}
A_B &\equiv \frac{4 A_e P_m(k_{max}) k_{max}^4}{27\pi^2} \\
&\approx 2 \times 10^{-6} \left(\frac{A_e}{10^{-4}}\right) \left(\frac{k_{max}}{400 \text{ Mpc}^{-1}}\right)^{n_s} \text{ Mpc}^{-1}.
\end{aligned}
\tag{A12}
$$

2. Second limit: $k_J < k_{max} \ll k$ ($x_J < x_{max} \ll 1$)

In the limit where $x_{max} \ll 1$, we approximate $\beta(x,\mu) \approx 1$ and therefore

$$
\begin{aligned}
I_x(k,\mu) &= \frac{4}{9} P_m(k) x_J^4 C_\alpha^{(1)}(k_{max}) x_{max}^{5+\alpha} \\
&\approx \frac{4}{9} P_m(k_{max}) x_{max/J}^{-4} C_\alpha^{(1)}(k_{max}) x_{max}^{13+\alpha-n_s}.
\end{aligned}
\tag{A13}
$$

Again, the μ integral in Eq. (A2) gives $4/3$, and we have

$$
I(k) = A_B C_\alpha^{(1)}(k_{max}) x_{max/J}^{-4} \left(\frac{k}{k_{max}}\right)^{n_s-6}.
\tag{A14}
$$

[1] D. Baumann and D. Green, Phys. Rev. D **85**, 103520 (2012).

[2] V. Assassi, D. Baumann, and D. Green, J. Cosmol. Astropart. Phys. 11 (2012) 047.

[3] X. Chen and Y. Wang, J. Cosmol. Astropart. Phys. 09 (2012) 021.

[4] T. Noumi, M. Yamaguchi, and D. Yokoyama, J. High Energy Phys. 06 (2013) 051.

[5] N. Arkani-Hamed and J. Maldacena, arXiv:1503.08043.

[6] H. Lee, D. Baumann, and G. L. Pimentel, J. High Energy Phys. 12 (2016) 040.

[7] S. Kumar and R. Sundrum, J. High Energy Phys. 05 (2018) 011.

[8] H. An, M. McAneny, A. K. Ridgway, and M. B. Wise, J. High Energy Phys. 06 (2018) 105.

[9] H. An, M. McAneny, A. K. Ridgway, and M. B. Wise, Phys. Rev. D **97**, 123528 (2018).

[10] D. Baumann, G. Goon, H. Lee, and G. L. Pimentel, J. High Energy Phys. 04 (2018) 140.

[11] S. Kumar and R. Sundrum, J. High Energy Phys. 04 (2019) 120.

[12] D. Anninos, V. De Luca, G. Franciolini, A. Kehagias, and A. Riotto, J. Cosmol. Astropart. Phys. 04 (2019) 045.

[13] J.-O. Gong, S. Pi, and M. Sasaki, J. Cosmol. Astropart. Phys. 11 (2013) 043.

[14] S. Pi and M. Sasaki, J. Cosmol. Astropart. Phys. 10 (2012) 051.

[15] C. Gordon and A. Lewis, Phys. Rev. D **67**, 123513 (2003).

[16] C. Gordon and J. R. Pritchard, Phys. Rev. D **80**, 063535 (2009).

[17] G. P. Holder, K. M. Nollett, and A. van Engelen, Astrophys. J. **716**, 907 (2010).

[18] A. D. Linde and V. F. Mukhanov, Phys. Rev. D **56**, R535 (1997).

[19] M. Sasaki, J. Valiviita, and D. Wands, Phys. Rev. D **74**, 103003 (2006).

[20] D. H. Lyth, C. Ungarelli, and D. Wands, Phys. Rev. D **67**, 023503 (2003).

[21] D. Langlois and A. Riazuelo, Phys. Rev. D **62**, 043504 (2000).

[22] C. He, D. Grin, and W. Hu, Phys. Rev. D **92**, 063018 (2015).

[23] A. De Simone and T. Kobayashi, J. Cosmol. Astropart. Phys. 08 (2016) 052.

[24] J. B. Muñoz, D. Grin, L. Dai, M. Kamionkowski, and E. D. Kovetz, Phys. Rev. D **93**, 043008 (2016).

[25] C. H. Heinrich, D. Grin, and W. Hu, Phys. Rev. D **94**, 043534 (2016).

[26] T. L. Smith, J. B. Muñoz, R. Smith, K. Yee, and D. Grin, Phys. Rev. D **96**, 083508 (2017).

[27] J. Valiviita, J. Cosmol. Astropart. Phys. 04 (2017) 014.

[28] Y. Akrami et al. (Planck Collaboration), Astron. Astrophys. **641**, A10 (2020).

[29] D. Grin, O. Dore, and M. Kamionkowski, Phys. Rev. D **84**, 123003 (2011).

[30] D. Grin, O. Dore, and M. Kamionkowski, Phys. Rev. Lett. **107**, 261301 (2011).

[31] D. Grin, D. Hanson, G. P. Holder, O. Doré, and M. Kamionkowski, Phys. Rev. D **89**, 023006 (2014).

[32] T. Haga, K. Inomata, A. Ota, and A. Ravenni, J. Cosmol. Astropart. Phys. 08 (2018) 036.

[33] J. Chluba and D. Grin, Mon. Not. R. Astron. Soc. **434**, 1619 (2013).

[34] N. Lee and Y. Ali-Haïmoud, Phys. Rev. D **104**, 103509 (2021).

[35] M. T. Soumagnac, R. Barkana, C. G. Sabiu, A. Loeb, A. J. Ross, F. B. Abdalla, S. T. Balan, and O. Lahav, Phys. Rev. Lett. **116**, 201302 (2016).

[36] M. T. Soumagnac, C. G. Sabiu, R. Barkana, and J. Yoo, Mon. Not. R. Astron. Soc. **485**, 1248 (2019).

[37] C. Heinrich and M. Schmittfull, Phys. Rev. D **100**, 063503 (2019).

[38] J. B. Muñoz, Phys. Rev. D **100**, 063538 (2019).

[39] J. B. Muñoz, Phys. Rev. Lett. **123**, 131301 (2019).

[40] S. C. Hotinli, T. Binnie, J. B. Muñoz, B. R. Dinda, and M. Kamionkowski, Phys. Rev. D **104**, 063536 (2021).

[41] A. Barreira, G. Cabass, D. Nelson, and F. Schmidt, J. Cosmol. Astropart. Phys. 02 (2020) 005.

[42] A. Barreira, G. Cabass, K. D. Lozanov, and F. Schmidt, J. Cosmol. Astropart. Phys. 07 (2020) 049.

[43] S. C. Hotinli, J. B. Mertens, M. C. Johnson, and M. Kamionkowski, Phys. Rev. D **100**, 103528 (2019).

[44] G. Sato-Polito, J. L. Bernal, K. K. Boddy, and M. Kamionkowski, Phys. Rev. D **103**, 083519 (2021).

[45] N. A. Kumar, S. C. Hotinli, and M. Kamionkowski, Phys. Rev. D **107**, 043504 (2023).

[46] S. Naoz and R. Narayan, Phys. Rev. Lett. **111**, 051303 (2013).

[47] T. Venumadhav, A. Oklopcic, V. Gluscevic, A. Mishra, and C. M. Hirata, Phys. Rev. D **95**, 083010 (2017).

[48] V. Gluscevic, T. Venumadhav, X. Fang, C. Hirata, A. Oklopcic, and A. Mishra, Phys. Rev. D **95**, 083011 (2017).

[49] N. Aghanim et al. (Planck Collaboration), Astron. Astrophys. **641**, A6 (2020); **652**, C4(E) (2021).

[50] R. H. Cyburt, B. D. Fields, K. A. Olive, and T.-H. Yeh, Rev. Mod. Phys. **88**, 015004 (2016).

[51] R. J. Cooke, M. Pettini, and C. C. Steidel, Astrophys. J. **855**, 102 (2018).

[52] Y. Ali-Haimoud and C. M. Hirata, Phys. Rev. D **83**, 043513 (2011).

[53] N. Lee and Y. Ali-Haïmoud, Phys. Rev. D **102**, 083517 (2020).

[54] J. Lesgourgues, arXiv:1104.2932.

[55] S. Naoz, N. Yoshida, and R. Barkana, Mon. Not. R. Astron. Soc. **416**, 232 (2011).

[56] S. Naoz and R. Barkana, Mon. Not. R. Astron. Soc. **362**, 1047 (2005).

[57] R. M. Kulsrud, *Plasma Physics for Astrophysics* (Princeton University Press, Princeton, New Jersey, 2004).

[58] T. Papanikolaou and K. N. Gourgouliatos, arXiv:2301.10045.

[59] J. M. Bardeen, J. R. Bond, N. Kaiser, and A. S. Szalay, Astrophys. J. **304**, 15 (1986).

[60] N. Sugiyama, Astrophys. J. Suppl. Ser. **100**, 281 (1995).

[61] A. D. Amaral, T. Vernstrom, and B. M. Gaensler, Mon. Not. R. Astron. Soc. **503**, 2913 (2021).

[62] K. L. Pandey and S. K. Sethi, Astrophys. J. **762**, 15 (2013).

[63] S. Chongchitnan and A. Meiksin, Mon. Not. R. Astron. Soc. **437**, 3639 (2014).

[64] R. Alves Batista and A. Saveliev, Astrophys. J. Lett. **902**, L11 (2020).

[65] M. Ackermann *et al.* (Fermi-LAT Collaboration), Astrophys. J. Suppl. Ser. **237**, 32 (2018).

[66] V. A. Acciari *et al.* (MAGIC Collaboration), Astron. Astrophys. **670**, A145 (2023).

[67] L. M. Widrow, Rev. Mod. Phys. **74**, 775 (2002).

[68] A.-C. Davis, M. Lilley, and O. Tornkvist, Phys. Rev. D **60**, 021301 (1999).